

Three-dimensional modelling and finite element analysis of the human mandible during clenching

AH Choi,* B Ben-Nissan,* RC Conway†

Abstract

Background: Until recently, very few papers have been published concerning the development, analysis and experimental verification of three-dimensional, finite element modelling of the human adult edentulous mandible. The purpose of this study was to improve the method of modelling by using computer-aided engineering (CAE) and computer-aided design (CAD) methods and to utilize the model in analyzing maxillofacial problems.

Methods: The model geometry was derived from position measurements taken from 28 diamond blade cut cross-sections of an average size human adult edentulous mandible and generated using a special sequencing method. Data on anatomical, structural, functional aspects and material properties were obtained from measurements and published data. The materials were idealized as transversely isotropic. The complete model consisted of 258 solid elements and 1635 nodes.

Results: The model was solved for displacements and stresses during clenching. In general, the observed displacement and stresses (tensile and compressive) were highest around the condylar region. Compressive stress was also observed around the premolar and molar bite points.

Conclusion: This investigation has shown that the use of computer-aided modelling in conjunction with the finite element analysis could be effectively utilized in biomechanical analysis of the mandible. It could help to investigate many functional problems and could reduce the time of extensive experimentations.

Key words: Finite element analysis, three-dimensional modelling, human mandible, clenching, muscle forces.

Abbreviations and acronyms: CAD = computer-aided design; CAE = computer-aided engineering; CT = computer-aided tomography; FEA = finite element analysis; IEMG = integrated electromyogram; PC = personal computer; TMJ = temporomandibular joint.

(Accepted for publication 2 July 2004.)

INTRODUCTION

Computer modelling and finite element analysis (FEA) have generated a great deal of interest since their inception. In particular, reaction to their use in the study of the human body has been extremely enthusiastic. Such studies have ranged from the analysis of various mechanical properties using simplistic two-dimensional models to the complex problem of the upper airway and its involvement in obstructive sleep apnoea. Of equal and challenging complexity is the study of the human mandible. No other bone combines such sophistication of shape with anatomical elements that include cortical and cancellous bone, dental tissues, ligaments, nerves, blood vessels and cartilage. In addition, the mandible also impacts directly on body aesthetics and functions, playing a pivotal role in speech, mastication, swallowing and facial expression. Unfortunately, the mandible is also often compromised by a vast array of pathological processes. Modelling can provide us with further understanding of the pathogenesis of these diseases and contribute toward our endeavours to provide suitable treatments.

Application of the finite element stress analysis technique to the biomechanical investigation of the oral systems, such as human teeth, periodontal ligament, implant designs and mandibular bone modelling, was initiated in the early 1970s.

The first three-dimensional mandible model that was symmetric about the median line was developed by Gupta *et al.*¹ The model geometry was derived from the physical measurements taken of a mandible. The idealized structure was reported to consist of 271 nodes and 240 solid elements. Knoell² attempted an improved three-dimensional model of the mandible. This model consisted of a three dimensional, finite element representation of one-half of a dried *in vitro* mandible that was symmetric about the symphysis but was constrained along the base of the mandible that did not allow accurate loading. The materials were idealized as homogeneous, isotropic, linearly elastic solids. The basic material properties for dentine and cortical bone were taken from the literature. The model was reported to consist of 674 nodes and 941 elements.

*Department of Chemistry, Materials and Forensic Science, University of Technology, Sydney.

†Department of Oral and Maxillofacial Surgery, Westmead Hospital, Westmead, New South Wales.

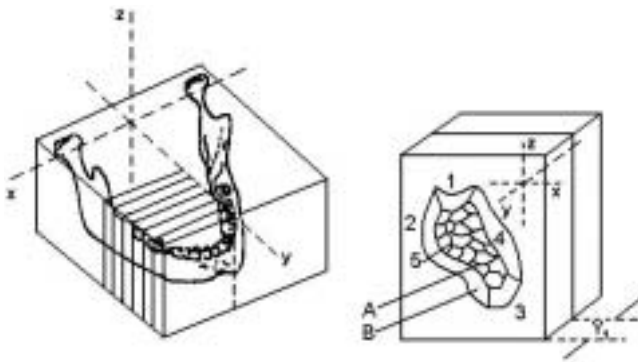


Fig 1. A typical cross-section of the mandible. Each cross-section of the bone was divided into five sections, the outer four representing the cortical bone and the inner one the cancellous bone, where numbers 1-4 represents cortical bone and number 5 represents cancellous bone; (A) cancellous bone; (B) cortical bone.

The first anatomically correct three-dimensional model was developed by Ben-Nissan *et al.*³ for the analysis of functional distortions. The complete model consisted of 1106 nodes and 258 solid elements.

A three-dimensional finite element model of a partially edentulous human mandible was generated by Hart⁴ to calculate the mechanical response to simulated isometric biting and mastication loads.

Korioth⁵ developed a three-dimensional finite element model of a human mandible reconstructed from tomographs of a dry dentate jaw. The final finite element model of the mandible consisted of 5580 nodes and 4572 elements. Different structures in the model were assigned material characteristics which were thought to conform to the best data available in literature.

The mathematical models used in most of these studies have been almost exclusively first-order, partially completed, over-constrained structural models, some exhibiting limited anatomic description and properties. Since structures in the oral cavity are complex by nature, the only useful mathematical models of the mandibular environment are those which represent these complexities.

Improvements implemented with this current model include forces acting on the mandible, realistic geometry and boundary conditions analogous to musculature support and ultimately better bone and tissue property characterization, both structurally and biologically. However, it has to be remembered it is extremely difficult to perform complete three-dimensional mechanical analysis of the mandible with its complex configuration. The use of computational modelling and analysis is essential if the analysis is to be applied to physiological problems. Although in the past large computational sources were required for this type of modelling, today a personal computer (PC) or a laptop with adequate power and appropriate basic tools can be readily used to aid the modelling with excellent ease and accuracy.

MATERIALS AND METHODS

A dry human adult edentulous mandible, judged by visual inspection to be normal, was used to define the

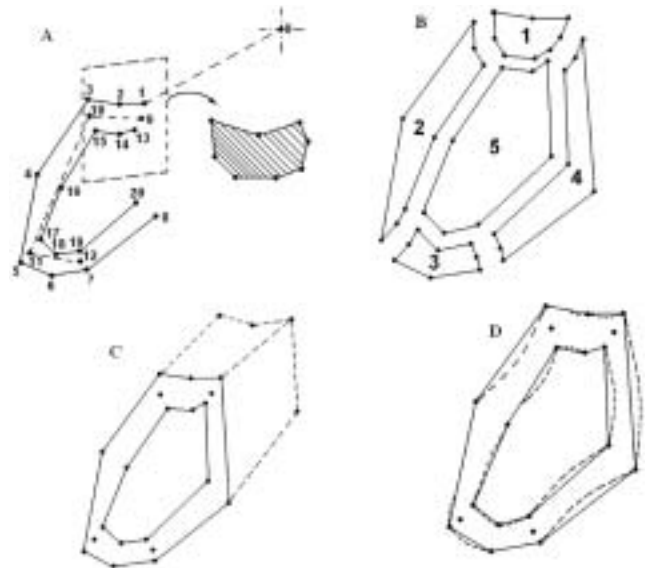


Fig 2. Nodal point generation using digitizer: (A) Digitizing sequence and wire frame diagram; (B) generation of surface planes of the brick elements; (C) element perimeter and midside nodes on cross-section; (D) element perimeter superimposed on real cross-section.

geometry of the model. The mandible was embedded in polyester resin, including a guide pin, which was positioned along the alveolar ridge to designate the 'origin' for a specific number sequencing method used during the modelling.

The mandible was then cross-sectioned vertically into 28 sections, using a diamond blade cutter to minimize bone loss (Fig 1). The cortical bone outlines, cancellous bone layers and reference points were traced onto drawing paper for one half of the symmetric structure. These outlines were then digitized by using a Summagraphics ID digitizer (The Logic Group, Austin, Texas, USA) and a specifically developed data-producing sequence. The wire-frame was developed using the original mandibular measurements and an additional subroutine was utilized to compensate for the bone loss during the cross-sectioning process and an anatomically correct model was developed.

An auto-drafting system and finite element programmes, first by MSC-Nastran (MSC Software, Sydney, Australia) and then the more simplified STRAND7 (G+D Computing Pty Ltd, Sydney, Australia) were used as the modelling algorithms for the work described in this paper.

Each cross-section of the bone was divided into five sections, the outer four representing the cortical bone and the inner one the cancellous bone (Fig 1). To model this composite, a number sequencing method was developed to match the finite element input data sequence (Fig 2). The sequencing method works by picking a number of points on each of the mandible cross-sections and numbering them consecutively, for example, numbers 1-8 represent the cortical bone outline and 13-20 represent the interface between cortical and cancellous bone to allow brick element mid-point arrangement. The brick elements contained 16 nodal points. The first element single face –

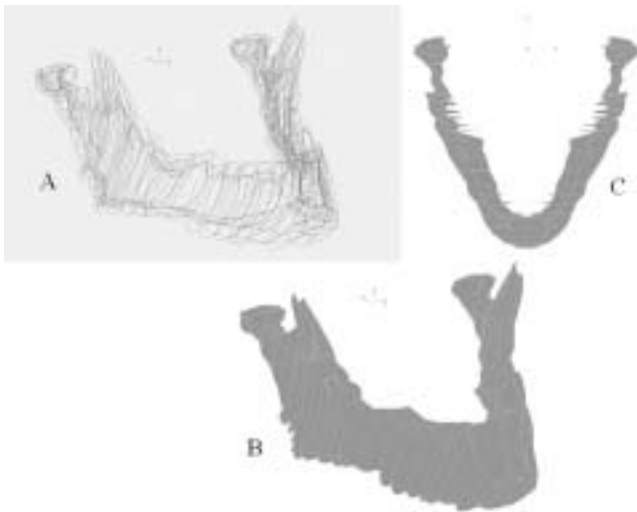


Fig 3. Three-dimensional finite element model of the human mandible. (A) Wire frame model showing the cortical bone outline and cancellous bone inner layer; (B) frontal view; (C) top view.

measured by a single cross-section – contained nodal numbers 1, 2, 3, 9, 10, 13, 14 and 15. Digitizing starts with the 'origin', designated 0; following points after that were digitized as 1-8, then 9-12 and finally 13-20. The same digitizing sequence was applied to the second cross-sectional plane and a subroutine was written to join these planes to generate the first five elements, four on the sides and one at the centre (Fig 2). The first four were assigned properties relating to the cortical bone and the centre element was assigned cancellous bone mechanical properties. The sequencing method is shown in Fig 1, 2.

The direction of the number sequencing is very important during this first stage of modelling as the wrong sequence can change the input data for the succeeding finite element work. Once the two-dimensional model has been completed, the cross-sections can be joined using the known thickness (y) values, obtained during the cross-sectioning of the mandible (Fig 1). As stated earlier a small subroutine was utilized during the joining process to compensate for the bone loss.

The three-dimensional model then was completed and once the obvious geometric faults had been identified and corrected, general co-ordinate data were generated. The generated data could then be compared with the bulk mandibular measurements and if the co-ordinate data were found satisfactory then the grid-point data were transferred to the Strand7 FEA package for further process. Reflecting the entire right hemimandible about the mid-sagittal plane from the symphysis to the origin of the xyz system (y -axis) then completed the final construction of the three-dimensional mandible model (Fig 1). The complete model consisted of 258 brick FEA elements and 1635 nodes (Fig 3).

Material properties

Data on the material properties of mandibular cortical and cancellous bones were taken from

Table 1. Mechanical properties used in finite element computations

Material	Young's modulus (GPa)			Poisson's ratio		
	E_1	E_2	E_3	ν_{12}	ν_{23}	ν_{13}
Cortical bone ^{10,11}	6.9	8.2	17.3	0.315	0.325	0.310
Cancellous bone ¹²	0.32	0.39	0.96	0.3	0.3	0.3

published data which were determined on small specimens obtained from the mandibles of cadavers by means of ultrasonic wave methods⁶⁻⁹ and other material testing techniques.^{10,11} The cortical and cancellous bone of the mandible can be considered to be transversely isotropic with a higher elastic modulus in the longitudinal direction and a lower elastic modulus in all transverse directions. Therefore, all the individual elements for both cortical and cancellous bone in our model were represented as transversely isotropic.

In this analysis the Young's Modulus and Poisson's ratio for the cortical bone were obtained from Arendts and Sigolotto^{10,11} and cancellous bone was obtained from Turner *et al.*¹² All material properties assigned to the structural elements are listed in Table 1.

Applied forces and boundary conditions

A feature of the FEA is that the reference plane for deformation must be defined to remove possible rigid body motion. For this analysis three nodes on the symmetry plane were fixed in space by the use of spring elements. Reactions of these points were shown to be zero so that restraining these parts had no effect on the stress distribution. Note that the model is completely free to deform, removing the approximation caused by over-restraining in the previously published models.^{1,2,4,5}

For the finite element model to be valid, the applied forces must be in equilibrium so that the reactions at the restrained nodes in the symphysis area will be zero. It was therefore necessary to define the physical conditions during various mandibular movements to reduce the complex force systems to a form that allowed the deformation of valid load cases for the finite element model. The non-vertical bite force (x and y components) and asymmetrical muscle forces were applied to this finite element model during the muscle force calculations stage under various functional mandibular loading. The only limitation for these biomechanical calculations is that the mandible must reach a condition of equilibrium. In other words, the moments generated by the sum of the applied muscle and bite forces must be equal to the moment generated by the reaction force(s) which in our case was applied at the condylar region. This was achieved by appropriate calculations prior to the application of the final FE boundary conditions.

The energy that moves the mandible and allows functioning of the masticatory system is provided by muscles. There are four pairs of muscles making up a group called the muscles of mastication: the masseter, temporalis, medial pterygoid and lateral pterygoid. Although previously ignored in the biomechanical

Table 2. Muscle actions of mastication

Muscles of mastication	Actions
Masseter	Elevation of the mandible
Temporalis	Elevation of the mandible
Medial pterygoid	Elevation and protrusion of the mandible
Lateral pterygoid	Protrusion of the mandible
Openers	Depression of the mandible

Table 3. Average length (mm) and weight (gr) of muscles of mastication (modified from Schumacher¹⁶)

Muscles	Average length (mm)		Average weight (gr)			
	Male	Female	Wet wght	%	Dry wght	%
Masseter	26.7	25.2	7.85	28.0	2.35	28.1
Temporalis	36.1	31.5	12.89	45.8	3.82	45.7
Medial pterygoid	17.7	14.9	3.13	11.1	0.92	11.1
Lateral pterygoid	22.8	21.5	4.24	15.1	1.26	15.1

analysis of the muscles of mastication, the digastrics also play an important role in mandibular depression (Table 2).

The muscle forces considered in the analysis were selected from Barbanel,¹³ Throckmorton and Throckmorton,¹⁴ Pruim *et al.*,¹⁵ and various physical measurements that were based on the physiological cross-sectional area.

All forces were assumed to be symmetrical and had equal magnitude on the right and left side of the mandible. The forces exerted by contracting muscles were represented by vectors in all three directions. Various investigators made similar assumptions. This assumption is reasonable when the muscle is homogeneous and acts as a whole.¹⁴

The direction of these vectors can be defined by the connecting lines between the centroids of the origins and the insertions of the muscles (Fig 4). Descriptions of these areas of attachments were derived from the anatomic literature¹⁶ and measurements on different skulls (Table 3).¹⁷

The force a muscle can exert is not only determined by physiological parameters (level of neuronal

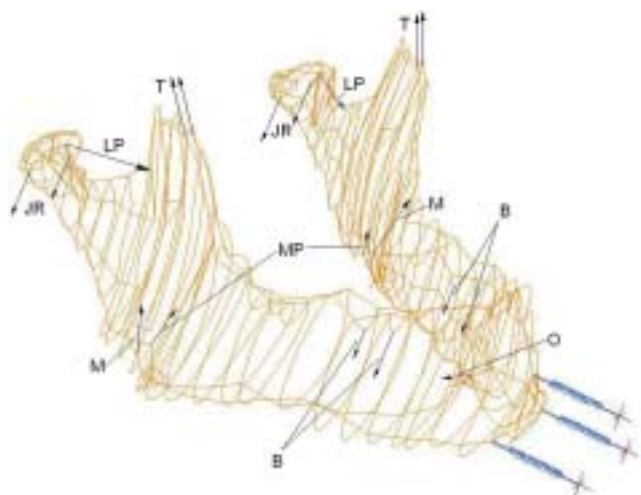


Fig 4. Applied forces during clenching. (M) Masseter; (MP) Medial pterygoid; (O) Openers; (LP) Lateral pterygoid; (B) Bite force; (T) Temporalis; (JR) Joint reaction force.

Table 4. Physiological cross-sectional area (cm²) of the facial muscles

Muscles	Pruim <i>et al.</i> ¹⁵	Schumacher ¹⁶	Ben-Nissan ¹⁷
Medial pterygoid	} 5.3†	1.97	2.0
Masseter		3.02	3.0
Temporalis	4.2*	3.81	3.8
Openers	1.0†	-	1.4
Lateral pterygoid	2.1†	1.83	1.8

*Includes anterior and posterior temporalis.

†Only digastric was measured.

Table 5. Averaged calculated maximum muscle forces (N) in each single muscle group and related standard deviations

Muscle	Carlsoo ^{18,19}	Schumacher ¹⁶	Pruim ¹⁴	Osborn ²⁰	Ben-Nissan ¹⁷
Medial pterygoid	299±46	190	} 639±176	254	191
Masseter	614±107	340		450	340
Ant temporalis	519±102	} 420	362±65	264	} 528
Post temporalis	305±102		197±26	323	
Openers	-	-	115±40	107	155
Lateral pterygoid	525	175	378±106	382	378

Table 6. Average maximum muscle tension (G) in (MPa)

Investigators	G (MPa)
Morris ²¹	0.9
Carlsoo ^{18,19}	1.1
Ikai and Fukunaga ²²	0.7
Pruim ¹⁵	1.4
Ben-Nissan ¹⁷	1.47

activation, speed of contraction, muscle length) but also by anatomical parameters, such as the total cross-section of all muscle fibres, the so-called physiological cross-section. The measured physiological cross-sectional area and the published data available¹⁶⁻¹⁸ were used to determine the forces of the various muscles (Tables 4-6). The data for the physiological cross-sectional areas, origins and insertions of the facial muscles were measured on various cadavers.¹⁷ The values of maximum muscle tension G, which directly relates to the maximum force exerted by a muscle to its physiological cross-sectional area, are provided in Table 6.¹⁵⁻²²

Two methods have been used to estimate the magnitude of the muscle forces. Several investigators¹⁵⁻¹⁷ have attempted to estimate the force generated by each muscle from the total cross-sectional area of the muscle. In the second method¹⁸⁻¹⁹ the integrated electromyogram (IEMG) from each muscle was used as an estimate of muscle force.

In order to carry out any analysis of jaw function it is necessary to know the lines of masticatory muscle actions and their moment arms (Tables 7 and 8).^{13-17,20,23} For the present study, the bite force (clench force) was directed at an angle of about 85° to the averaged occlusal plane. Each bite force was divided between the second premolar and the first molar symmetrically placed with respect to the midsagittal plane, thus simulating the work of Pruim *et al.*¹⁵ During clenching,

Table 7. Muscle moment arms (cm)

Muscle	Barbenel ¹³		Grant ²³		Pruim ¹⁵	
	ICR*				Centre of condyle	
	Rest	Open	Rest	Open		
Med pterygoid	2.3	4.5	0.45	2.4	2.2	3.5
Masseter	2.7	5.4	0.95	3.3	2.95	4.1
Ant temporalis	} 2.6	5.8	5.2	3.4	3.1	3.3
Post temporalis		3.5	6.3	1.9	1.5	2.1
Openers	-	-	-	-	-	10.4
Lat pterygoid	-	-	-	-	-	-

*Instantaneous centre of rotation.

Table 8. Angular directions (degrees)

Muscle	Pruim ^{15*}	Osborn ²⁰	Throckmorton ¹⁴	Ben-Nissan ¹⁷
Med pterygoid	70.3	55, 67	-	80
Masseter	64.14	72, 75, 87, 91	66	80
Ant temporalis	99.5	} 98, 12, 144	} 112	} 113.4
Post temporalis	139.8			
Openers	210.8	190	-	210.8
Lat pterygoid	-	10, 332, 356	-	348

*Measured when condyle was located opposite the tubercle and not in the articular fossa.

all muscles were assumed to be active. Calculated muscle forces are presented in Table 9. The reaction forces were assumed to be acting at the centre of the condyles (Fig 4).

Finite element analysis was performed under non-linear static conditions due to the complex constitutive laws of material behaviour, which is programmed automatically using a commercially available FEA package STRAND7.

RESULTS

To maximize the model accuracy, a comparison has been made between this computer-generated model with the bulk mandibular measurements, which fall within published measurements.

Figure 5 shows the models for clenching in the mandible's undeformed and deformed states. The undeformed state depicts the model with its structural elements in their unloaded condition and is represented by the wire frame structure. The deformed state represents a state in which the muscular loads have displaced the structural elements and the model has reached a state of static equilibrium, represented in grey.

The distortion of the mandible during clenching is shown in Fig 6 with the use of contour plots. Distortion values were found to be in the range of 0.05-0.3mm around the premolar to the third molar regions.

Table 9. Calculated force (N) acting on the mandible during clenching (one side only)¹⁷

Muscles	Force (N)
Bite force	403.7
Joint reaction force	471.9
Lateral pterygoid	378.0
Masseter	340.0
Medial pterygoid	191.4
Openers	155.9
Temporalis	528.6

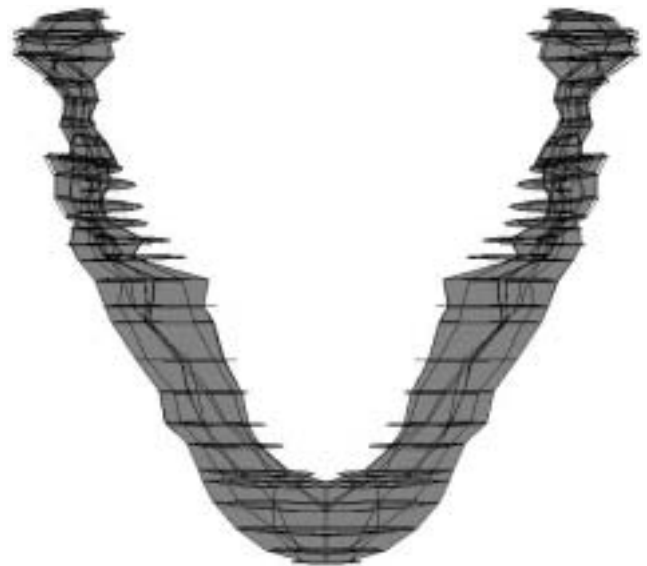


Fig 5. Deformed and undeformed state of the mandible during clenching (top view). The deformed state is represented in grey.

Maximum distortions were recorded around the condylar and third molar regions. Although various clinical measurements were reported during the mandibular opening, there are no clinical distortion data available during the clenching function.

The distribution of tensile and compressive stress is shown in Fig 7, 8. Regions experiencing high magnitudes of tensile stress included the areas around the condylar region and extended to the third molar region, while high magnitudes of compressive stress were experienced in areas around the condylar region, extending to the coronoid process and also around the premolar and molar bite points.

DISCUSSION

This model can be used for various mandibular functional movements, such as opening, protrusion and biting. Due to the power of new-generation PCs and laptops and the availability of compact but powerful FEA packages, the model can be adapted to a PC that can be used to analyze functional movements by the dental practitioner. Although this model was generated using simple and basic modelling tools, it can be easily modified by using individual patient jaw geometry

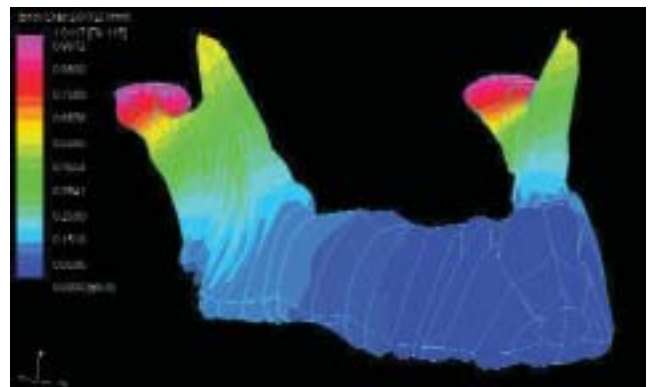


Fig 6. Distortion observed on the mandible (right lateral front view).

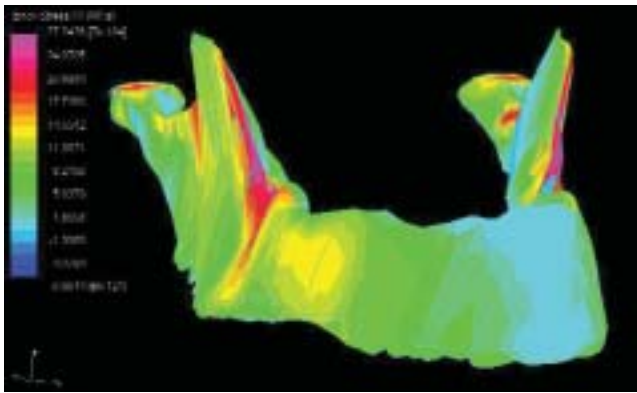


Fig 7. Tensile stress acting on the mandible (right lateral front view).

obtained from computer-aided tomography (CT) scans to simulate personal mandibular models.

Our three-dimensional FEA model of the human adult edentulous mandible is unique. Its strengths lie in the fact that it is a simple process that utilizes a cross-sectional sequencing method that accurately reproduces the mandible not only in geometry and morphology but also, most importantly, in structure.

There have been various investigations into the stresses in the mandibular bone during various loading tasks.^{5,17,24,25} The tensile stress recorded on the mandibular bone ranged from 25-121MPa, while the compressive stress ranged from 0.3-167MPa. There are no specific guidelines in the literature for interpreting the results of neither stress analysis, nor the kind and range of stresses that must be present or allowed.

According to Ben-Nissan,¹⁷ who used a mainframe computer, the distortion of the mandible recorded at the second molar region was reported to be 0.15mm, compared to 0.1518mm obtained from this current work using a PC. However, displacement values of 0.32-0.51mm around the second molars during wide opening movement and 0.432-0.71mm during protrusion reported showed higher distortion values in comparison to clenching function. There is a good agreement between the calculated values and the work published by Ben-Nissan.¹⁷

Use of this computerized modelling methodology will have innumerable applications in both dentistry and surgery, at not only a research but also at a clinical level.

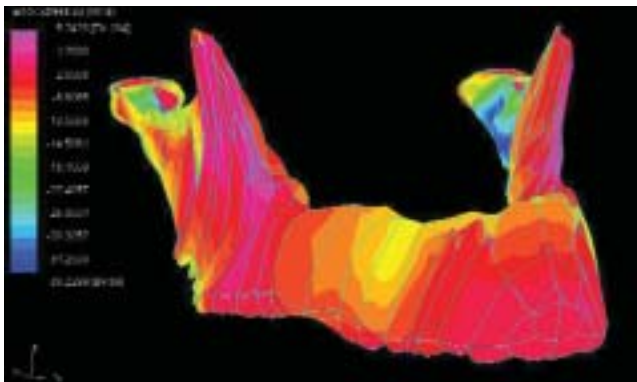


Fig 8. Compressive stress acting on the mandible (right lateral front view).

For example, the ability to take an individual patient's data from their CT scan or other appropriate imaging to produce his or her own model will be possible. This model can then be used in the following applications:

Dental implants

It will be possible to assess the correct number, location, configuration and size of implants required to address that person's restorative and functional needs. For example, the dentist will be able to predict the functional loads that an implant supported cantilevered bridge restoration may develop. In doing so, he or she can plan any necessary implant surgery in order to predictably provide support for the potential loads, thereby minimizing failure or, conversely, over-treatment.

Pathology resection and reconstruction

Reconstructions after the resection of various pathologies involving the mandible will be able to be more predictably performed so that form and function are returned as closely as possible to the pre-morbid state.

Traumatology

Accurate three-dimensional modelling will enable the clinician to best assess the form and engineering requirements of hardware that is used to treat mandibular fractures so that both reduction and fixation of the fracture can be obtained whilst minimizing osteosynthesis plate size, number and bulk.

Aesthetic facial surgery

Not only can surgical planning be refined with this technology, it can also be used to study various aspects of facial bone osteotomies such as post-operative functional change and stability of the orthognathic movements.

Distraction osteogenesis

The success of distraction osteogenesis of the mandible depends upon accurate planning of the distraction vector required to produce the final position of the distracted segment. At present, planning methodology is rudimentary and struggles with even the unidirectional devices that are most commonly in use today. The use of our modelling concept could be used to refine this planning process, especially as intraoral multi-directional distraction devices become available.

Restorative dentistry

In a similar vein, to implant restorations various restorative tooth options could be analyzed under simulated functional loading and designed to resist these loads prior to manufacture.

Temporomandibular joint (TMJ) surgery

In recent years TMJ prostheses have received intense scrutiny due to failures that have primarily resulted from material failure. It is hoped that through further

design and materials improvement these prostheses can be improved so that the patient requiring TMJ replacement can benefit. Modelling technology may also contribute to perfecting prosthesis design and be used to assist *in vitro* testing so that the damages caused in the past produced by various materials failures can be avoided.

Research

From the preceding points it is evident that there are many areas in dentistry, materials science and other specialties involving the management of the facial skeleton and TMJ that require further extensive research which will benefit patient care. The development of our model can contribute significantly to these research processes.

CONCLUSION

The biomechanical events, that accompany functional loading of the human mandible, are not fully understood. The techniques normally used to record them are highly invasive. Finite element modelling offers a promising alternative approach in this regard, with the additional ability to predict regional stresses and strains in inaccessible locations. In this paper we have shown that the use of CAD and CAE in conjunction with FEA can provide a sophisticated tool for modelling complex anatomical structures.

ACKNOWLEDGEMENTS

The authors would like to express their gratitude to Emeritus Professor NL Svennsson and Professor DW Kelly from the University of New South Wales for their help and guidance and to Ms P Skinner for her time in reviewing the paper.

REFERENCES

1. Gupta KK, Knoell AC, Grenoble DE. Mathematical modeling and structural analysis of the mandible. *Biomater Med Devices Artif Organs* 1973;1:469-479.
2. Knoell AC. A mathematical model of an *in vitro* human mandible. *J Biomech* 1977;10:159-166.
3. Ben-Nissan B, Svennsson NL, Kelly DW, Vajda TT. Computer aided three-dimensional modeling and finite element analysis of the mandible. In: Williams JF and Stevens LK, eds. *Finite Element Methods in Engineering*. The University of Melbourne, 1987:290-294.
4. Hart RT, Hennebel VV, Throngpreda N, Van Buskirk WC, Anderson RC. Modeling the biomechanics of the mandible: a three-dimensional finite element study. *J Biomech* 1992;25:261-286.
5. Koriath TW, Romilly DP, Hannam AG. Three-dimensional finite element stress analysis of the dentate human mandible. *Am J Phys Anthropol* 1992;88:69-96.
6. Ashman RB, Van Buskirk WC. The elastic properties of a human mandible. *Adv Dent Res* 1987;1:64-67.
7. Dechow PC, Nail GA, Schwartz-Dabney CL, Ashman RB. Elastic properties of human supraorbital and mandibular bone. *Am J Phys Anthropol* 1993;90:291-306.
8. Ashman RB, Van Buskirk WC. The elastic properties of a human

- mandible. *Adv Dent Res* 1987;1:64-67.
9. Pithioux M, Lasaygues P, Chabrand P. An alternative ultrasonic method for measuring the elastic properties of cortical bone. *J Biomechanics* 2002;35:961-968.
10. Arendts FJ, Sigolotto C. Standard measurements, elasticity values and tensile strength behavior of the human mandible, a contribution to the biomechanics of the mandible – I. *Biomed Technik* 1989;34:248-255.
11. Arendts FJ, Sigolotto C. Mechanical characteristics of the human mandible and study of *in vivo* behavior of compact bone tissue, a contribution to the description of biomechanics of the mandible – II. *Biomed Technik* 1990;35:123-130.
12. Turner CH, Cowin SC, Rho JY, Ashman RB, Rice JC. The fabric dependence of the orthotropic elastic constants of cancellous bone. *J Biomech* 1990;23:549-561.
13. Barbenel JC. The biomechanics of the temporomandibular joint: A theoretical study. *J Biomech* 1972;5:251-256.
14. Throckmorton GS, Throckmorton LS. Quantitative calculations of temporomandibular joint reaction force – I. The importance of the magnitude of the jaw muscle forces. *J Biomech* 1985;18:445-452.
15. Pruim GJ, de Jongh HJ, ten Bosch JJ. Forces acting on the mandible during bilateral static bite at different bite force levels. *J Biomech* 1980;13:755-763.
16. Schumacher GH. *Functionelle Morphologie der Kaumuskelatur*. VEB Gustav Fischer Verlag: Jena, 1961.
17. Ben-Nissan B. Three dimensional modelling and finite element distortion analysis of the mandible. Sydney: University of New South Wales, 1987. PhD thesis.
18. Carlsoo S. Nervous co-ordination and mechanical function of the mandibular elevators; an electromyographic study of the activity, and an anatomic analysis of the mechanics of the muscles. *Acta Odont Scand* 1952;10:1-132.
19. Carlsoo S. Motor units and action potentials in masticatory muscles; an electromyographic study of the form and duration of the action potentials and an anatomic study of the size of the motor units. *Acta Morph Neerl Scand* 1958;2:13-19.
20. Osborn JW, Baragar FA. Predicted pattern of human muscle activity during clenching derived from a computer assisted model: symmetric vertical bite forces. *J Biomech* 1985;18:599-612.
21. Morris CB. The measurement of the strength of muscle relative to the cross-section. *Res Q Am Assoc Hlth Phys Educ* 1948;19:295-303.
22. Ikai M, Fukunaga T. Calculation of muscle strength per unit cross-sectional area of human muscle by means of ultrasonic measurement. *Int Z Angew Physiol* 1968;26:26-32.
23. Grant PG. Biomechanical significance of the instantaneous center of rotation: the human temporomandibular joint. *J Biomech* 1973;6:109-113.
24. Akca K, Iplikcioglu H. Finite element stress analysis of the influence of staggered versus straight placement of dental implants. *Int J Oral Maxillofac Implants* 2001;16:722-730.
25. Hirabayashi M, Motoyoshi M, Ishimaru T, Kasai K, Namura S. Stresses in mandibular cortical bone during mastication: biomechanical considerations using a three-dimensional finite element method. *J Oral Sci* 2002;44:1-6.

Address for correspondence/reprints:

Associate Professor B Ben-Nissan
 Department of Chemistry, Materials and Forensic
 Science, University of Technology, Sydney
 PO Box 123, Broadway, New South Wales 2007
 Email: b.ben-nissan@uts.edu.au